Original article

Nuclear Medicine Communications

Synthesis of ^{99m}Tc-EC-AMT as an imaging probe for amino acid transporter systems in breast cancer

Fan-Lin Kong[a], YinHan Zhang[a], Mohammad S. Ali[a], Chanksok Oh[a], Richard Mendez[a], Saady Kohanim[a], Ning Tsao[a], Mithu Chanda[a], Wen-Chien Huang[b] and David J. Yang[a]

Objective **This study was to develop a ^{99m}Tc-labeled α-methyl tyrosine (AMT) using L,L-ethylenedicysteine (EC) as a chelator and to evaluate its potential in breast tumor imaging in rodents.**

Methods **EC-AMT was synthesized by reacting EC and 3-bromopropyl AMT (N-BOC, ethyl ester) in ethanol/potassium carbonate solution. EC-AMT was labeled with ^{99m}Tc in the presence of tin (II) chloride. Rhenium-EC-AMT (Re-EC-AMT) was synthesized as a reference standard for ^{99m}Tc-EC-AMT. To assess the cellular uptake kinetics of ^{99m}Tc-EC-AMT, 13 762 rat breast cancer cells were incubated with ^{99m}Tc-EC-AMT for 0–2 h. To investigate the transport mechanism, the same cell line was used to conduct the competitive inhibition study using L-tyrosine. Tissue distribution of ^{99m}Tc-EC-AMT was determined in normal rats at 0.5–4 h. Planar imaging of breast tumor-bearing rats was performed at 30 and 90 min. The data were compared with those of ^{18}F-2-fluoro-2-deoxy-glucose. Blocking uptake study using unlabeled AMT was conducted to investigate the transport mechanism of ^{99m}Tc-EC-AMT *in vivo*.**

Results **Structures of EC-AMT and Re-EC-AMT were confirmed by nuclear magnetic resonance, high performance liquid chromatography and mass spectra. In-vitro cellular uptake of ^{99m}Tc-EC-AMT in 13 762 cells was increased as compared with that of ^{99m}Tc-EC and could be inhibited by L-tyrosine. Biodistribution in normal rats showed high in-vivo stability of ^{99m}Tc-EC-AMT. Planar scintigraphy at 30 and 90 min showed that ^{99m}Tc-EC-AMT could clearly visualize tumors. ^{99m}Tc-EC-AMT uptake could be significantly blocked by unlabeled AMT *in vivo*.**

Conclusion **The results indicate that ^{99m}Tc-EC-AMT, a new amino acid transporter-based radiotracer, is suitable for breast tumor imaging. *Nucl Med Commun* 31:699–707**

Nuclear Medicine Communications 2010, **31**:699–707

Keywords: amino acid transporter, breast cancer, EC-AMT, FDG, planar imaging

Departments of [a]Experimental Diagnostic Imaging and [b]Molecular and Cellular Biology, The University of Texas M.D. Anderson Cancer Center, Holcombe Boulevard, Houston, Texas, USA

Correspondence to Fan-Lin Kong, BS, Department of Experimental Diagnostic Imaging, Box 59, The University of Texas M.D. Anderson Cancer Center, 1515 Holcombe Boulevard, Houston, Texas 77030, USA
Tel: +1 713 745 7043; fax: +1 713 794 5456;
e-mail: fanlin.kong@mdanderson.org

Received 10 December 2009 **Revised** 19 February 2010
Accepted 17 March 2010

Introduction

Positron emission tomography (PET), using ^{18}F-2-fluoro-2-deoxy-glucose (FDG), is a gold standard for tumor detection and staging. Unfortunately, FDG has several limitations that give rise to false positive/negative diagnosis and poor predictive value of tumor response to chemo/radio therapy [1]. FDG has poor contrast in brain tumor because of the high uptake of glucose in both normal and neoplastic brain tissues [2], and it has poor differentiation of tumor from inflammatory tissue because of the high uptake of FDG in granulocytes and macrophages [3,4]. Radiolabeled amino acids show relatively low accumulation in normal tissues, rather high accumulation in tumor tissue, and rapid blood clearance. These radiolabeled amino acids are attractive as the main determinant of their uptake are amino acid transporters that are upregulated in cancer cells [5,6]. Upregulated amino acid transporters indirectly reflect elevated cell proliferation [7], and assessment of their activities promises potential applications in differential diagnosis and prediction of early treatment response. Among all the radiolabeled amino acids, aromatic amino acids are more suitable for tumor imaging because of easier chemical modification and characterization. However, aromatic amino acids tend to be decarboxylated [8], which reduces their ability to enter cells through amino acid transporters. Placing a methyl group at the α position could slower their metabolism; thus, greater effort was directed towards the ^{18}F-labeled and $^{123/124}$I-labeled aromatic amino acids such as 2-[^{18}F]fluoromethyl-L-phenylalanine [9], 2 and 3-L-[^{18}F]fluoro-α-methyl tyrosine (FAMT) [10–12], and ^{123}I-labeled L-3-[^{123}I]iodo-α-methyltyrosine [13].

Clinical study in lung cancer patients showed that FAMT had no false positives in the detection of primary tumors and lymph node metastases, and was able to improve the

0143-3636 DOI: 10.1097/MNM.0b013e328339ea48

diagnostic performance in nonsmall cell lung cancer [11]. FAMT has been proven to be transported into the tumor cells solely through the L-type amino acid transporter system (LAT), especially the LAT1 subtype [5]. LAT is the only system that can transport large neutral amino acids with aromatic rings such as tyrosine, phenylalanine and tryptophan [14,15]. LAT family is known to form heterodimers, which contain a chaperone-like heavy chain 4F2hc and a 12-time transmembrane light chain that is unique to each subtype [16]. Earlier clinical studies showed that uptake of FAMT in tumors was closely correlated with LAT1 expression and cell proliferation [11]. Although FAMT-PET shows very promising clinical results, the radiosynthetic yield is relatively low and the cost of using PET isotope ^{18}F is prohibitive. Therefore, it is desirable to develop a radiotracer with a simpler chemistry and affordable isotope, which can be used clinically in most major medical facilities.

Technetium-99m (^{99m}Tc) is an ideal radioisotope for diagnostic imaging studies because of its physical characteristics. It emits a 140 keV γ-ray in 89% abundance [17], which is commonly used by single photon emission computed tomography. The half-life of ^{99m}Tc is 6.02 h, which can provide serial images and therefore overcome the drawback of ^{18}F. Diaminodithiol compounds are known to form considerably stable Tc(V) O-complexes owing to the efficient binding of the oxotechnetium group to two thiols and two amine nitrogen atoms [18]. L, L-ethylenedicysteine (EC) is the most successful example of diaminodithiol chelates [19,20]. We reported earlier that EC conjugates through a peptide bond can be labeled with ^{99m}Tc efficiently with high radiochemical purity and the complex remains stable for several hours [20]. Here, we report the synthesis of ^{99m}Tc-labeled α-methyl tyrosine (AMT) using EC as a chelator and the evaluation of its potential use in breast tumor imaging.

Materials and methods

Chemicals and analysis

EC was purchased from Taiwan Hopax Chems, Mfg, Co., Ltd. (Kaohsiung, Taiwan). All other chemicals of analytical grades and solvents of high-performance liquid chromatography (HPLC) grade were obtained from Sigma-Aldrich (St Louis, Missouri, USA). Nuclear magnetic resonance (NMR) was performed on the Bruker 300 MHz Spectrometer and mass spectra were performed on the Waters Q-TOF Ultima Mass Spectrometer (Milford, Massachusetts, USA) at the core facility at the University of Texas MD Anderson Cancer Center (UTMDACC; Houston, Texas, USA). Chemical shifts were reported in δ (ppm) and *J* values in hertz. Sodium pertechnetate ($Na^{99m}TcO_4$) was obtained from a ^{99}Mo/^{99m}Tc generator by Mallinckrodt (Houston, Texas, USA). FDG was obtained from the Department of Nuclear Medicine at UTMDACC.

Synthesis of precursor *O*-[3-(*N*-ethylenedicysteine) propyl]-α-methyl tyrosine

Alpha-methyl tyrosine ethylester (compound 1)

Thionyl chloride (18 ml; 0.24 mol) was added to α-methyl-tyrosine (15.0 g; 0.08 mol) in anhydrous ethanol (100 ml) at 0°C. The mixture was refluxed at 80–90°C overnight with stirring. After cooling, the solvent was evaporated *in vacuo* to dryness. A saturated solution of $NaHCO_3$ (150 ml) was added to the residue. The white solid was filtered and washed with water, and recrystallized in ethanol and water to yield 15.7 g (91.7%). MS (*m/z*): 224.23 $[M]^+$.

N-t-butoxycarbonyl-α-methyltyrosine ethyl ester (compound 2)

Compound 1 (15.48 g; 69.35 mmol) was dissolved in anhydrous dichloromethane (200 ml). Di-tert-butyl dicarbonate (15.14 g; 69.35 mmol) and $NaHCO_3$ (58.3 g, 0.69 mol) were added. The reaction mixture was stirred overnight at 50°C, and the white solid was removed by filtration. The solution was washed with water and dried over anhydrous $MgSO_4$. The product was purified by column chromatography using a silica gel column and eluted with hexane/ethyl acetate (5 : 2 v/v) to yield 8.97 g (40%). MS (*m/z*): 346.16 $[M + Na]^+$.

N-t-butoxycarbonyl-O-[3-Br-propyl]-α-methyl tyrosine ethylester (compound 3)

Compound 2 (9.42 g; 0.029 mol) was dissolved in acetone (200 ml). 1,3-Dibromopropane (11.0 ml; 0.115 mol) and K_2CO_3 (10.0 g; 0.178 mol) were added under nitrogen. The reaction mixture was refluxed at 70–80°C overnight. After cooling and filtration, the solvent was removed under reduced pressure and the residue was dissolved in chloroform. The residue was washed with water and dried with anhydrous $MgSO_4$. The product was purified by column chromatography using a silica gel column and eluted with hexane/ethyl acetate (4 : 1 v/v) to yield 11.0 g (86%). MS (*m/z*): 445.10 $[M]^+$.

N-t-butoxycarbonyl-O-[3-(N-ethylenedicysteine) propyl]-α-methyl tyrosine (compound 4)

EC (3.33 g, 12.4 mmol) was dissolved in water (50 ml), and the pH was adjusted to 9-10 by NaOH (1 N). Compound 3 (3.86 g, 8.69 mmol) in ethanol (80 ml) was added to the above solution, followed by adding K_2CO_3 (8.6 g, 62.2 mmol). The reaction mixture was then heated at 90°C overnight. After cooling, the solvent was removed under reduced pressure and the residue was dissolved in chloroform (50 ml). The residue was washed with water, dried with anhydrous $MgSO_4$ and evaporated to dryness. Without further purification, compound 4 was used for the following steps.

O-[3-(N-ethylenedicysteine) propyl]-α-methyl tyrosine (compound 5)

The crude product of compound 4 (2.5 g, 0.04 mol) was dissolved in dichloromethane (50 ml). Hydrobromic acid

(48%, 4.5 ml) was added drop-wise to the solution over a 30 min-period at room temperature with stirring. After filtration, the white solid was washed with ethanol and recrystallized in water to yield 2.08 g (86%).

Rhenium-O-[3-(N-ethylenedicysteine) propyl]-α-methyl tyrosine (compound 6)

An ethanol solution (10 ml) containing trichlorooxobis (triphenylphosphine) rhenium(V) (110 mg, 0.13 mmol) was added to an aqueous solution (10 ml) with *O*-[3-(*N*-ethylenedicysteine) propyl]-α-methyl tyrosine (EC-AMT) (66 mg, 0.13 mmol) and potassium hydroxide (120 mg, 1.3 mmol), followed by refluxing at 90°C for 1 h. The color of reaction mixture changed from green to yellow. After cooling and filtration, the ethanol was removed *in vacuo*. The remaining aqueous solution was acidified to pH 4 with 1 N HCl. The yellow solid product rhenium (Re)-EC-AMT formed immediately was collected and recrystallized from water. MS (*m/z*): 739.29 $[M + HCl]^+$.

Radiolabeling of EC-AMT and EC with ^{99m}Tc

EC-AMT (1 mg) was dissolved in 0.2 ml sterile water, followed by adding tin(II) chloride (0.1 ml, 1 mg/ml). For EC labeling, EC (0.5 mg) was dissolved in 0.2 ml sterile water by adding 10 µl of 1 N NaOH (pH = 9). The required amount of $Na^{99m}TcO_4$ was added to EC or EC-AMT solution (pH 7.4). Radiochemical purity was determined by radio-HPLC (Waters, Milford, Massachusetts, USA) and eluted with acetonitrile:water (7 : 3) using a flow rate of 0.5 ml/min.

In-vitro cellular uptake of ^{99m}Tc-EC-AMT

The rat breast tumor cell line 13 762 (American Type Culture Collection, Rockville, Maryland, USA) was selected because the same cell line was used to create the animal model for in-vivo evaluation. The cells were maintained in Dulbecco's modified Eagle's medium and nutrient mixture F-12 Ham (DMEM/F12; GIBCO, Grand Island, New York, USA) at 37°C in a humidified atmosphere containing 5% CO_2. Cells were plated onto six-well tissue culture plates (2×10^5 cells/well) and incubated with ^{99m}Tc-EC-AMT (0.05 mg/well, 8 µCi/well), ^{99m}Tc-EC (0.025 mg/well, 8 µCi/well) or FDG (8 µCi/well) for 0–2 h. After incubation, the cells were washed with ice-cold PBS twice and detached by adding 0.5 ml of trypsin. The cells were then collected and the radioactivity was measured with a γ-counter (Cobra Quantum; Packard, Minnesota, USA). Data were expressed in mean ± SD percentage of cellular uptake (%Uptake).

Competitive inhibition study of ^{99m}Tc-EC-AMT

To investigate the transport mechanisms of ^{99m}Tc-EC-AMT, the competitive inhibition study using L-tyrosine was conducted. Rat breast tumor cells were co-incubated with ^{99m}Tc-EC-AMT (8 µg/well, 8 µCi/well) and L-tyrosine or ^{99m}Tc-EC (4 µg/well, 8 µCi/well) and L-tyrosine for 1 h. A set of concentrations of L-tyrosine (1x, 10x, 50x, and 100x of the ^{99m}Tc-EC-AMT concentration) were used. After incubation, the cells were washed with ice-cold PBS twice and detached by adding 0.5 ml of trypsin. The cells were then collected and the radioactivity was measured by a γ-counter. Data were expressed in mean ± SD %Uptake.

In-vivo tissue distribution studies

All animal studies were carried out in the Small Animal Imaging Facility at UTMDACC under a protocol approved by the Institutional Animal Care and Use Committee. Tissue distribution studies of ^{99m}Tc-EC-AMT (study I, $n = 9$), FDG (study II, $n = 9$) or ^{99m}Tc-EC (study III, $n = 9$) were conducted by using normal female Fischer 344 rats (150 ± 25 g, $n = 18$) (Harlan Sprague–Dawley, Indianapolis, Indiana, USA). For each compound, the rats were divided into three groups for three time intervals (0.5, 1, 4 h for ^{99m}Tc-EC-AMT and ^{99m}Tc-EC; 0.5, 1, 2 h for FDG; $n = 3$/time point). The injection activity was 25 ± 0.5 µCi/rat intravenously. At each time interval, the rats were killed and the selected tissues were excised, weighed and counted for radioactivity by a γ-counter. Each sample was calculated as percentage of the injected dose per gram of tissue wet weight. Counts from a diluted sample of the original injection were used as reference.

Planar scintigraphy and micro-PET imaging studies

Female Fischer 344 rats were inoculated subcutaneously with 0.1 ml of breast tumor cells 13 762 suspension (10^5 cells/rat) into the right legs. Planar scintigraphic imaging of ^{99m}Tc-EC-AMT and ^{99m}Tc-EC, or micro-PET imaging of FDG performed 12–14 days after inoculation, when the tumors reached approximately 1 cm in diameter. Planar scintigraphic images were obtained using M-CAM (Siemens Medical Solutions, Hoffman Estates, Illinois, USA) equipped with a low-energy high-resolution collimator. Anesthetized breast tumor-bearing rats were injected intravenously with ^{99m}Tc-EC-AMT (0.3 mg/rat, 300 µCi/rat; $n = 3$) or with ^{99m}Tc-EC (0.15 mg/rat, 300 µCi/rat; $n = 3$), respectively. The images were acquired up to 4 h after the administration of tracers. Computer-outlined regions of interest (in counts per pixel) between the tumor and muscle were used to calculate tumor/muscle (T/M) ratios. Micro-PET imaging of FDG was performed using an R4 micro-PET scanner (Concorde Microsystems, Tennessee, USA). The rats were injected intravenously with FDG (500 µCi/rat), and whole body images were acquired at 45 min. PET images were reconstructed by using the ordered subset expectation maximization algorithm.

In-vivo uptake blocking studies

To ascertain whether ^{99m}Tc-EC-AMT uptake is mediated specifically by LAT, in-vivo blocking studies using the unlabeled AMT as the competitive inhibitor were conducted. The same animal model used in the planar imaging studies was used. Unlabeled AMT (50 mg/kg)

dissolved in 0.3 ml saline was administered intravenously to mammary tumor-bearing rats 1 h before the ^{99m}Tc-EC-AMT injection. Planar scintigraphic images were acquired up to 4 h, and regions of interest of the tumor, muscle, liver, and kidneys were used to calculate the ratios of liver/muscle, kidney/muscle, and T/M, respectively. The results were compared with those from the rats injected with ^{99m}Tc-EC-AMT alone (control).

Results

Chemistry

EC-AMT was synthesized through a five-step procedure. The synthetic scheme is shown in Fig. 1. The structures and purities of EC-AMT and Re-EC-AMT were confirmed by ^{1}H-NMR and ^{13}C-NMR, mass spectra, and HPLC. For EC-AMT, the ^{1}H-NMR and ^{13}C-NMR results are ^{1}H-NMR (D_2O, δ/ppm): 7.10 (d, 2H, phenyl ring), 6.79 (d, 2H, phenyl ring), 3.96 (dd, 2H, O-CH2), 3.09 (t, 1H, CHN), 2.87 (d, 2H, $PhCH_2$-), 2.68–2.40 (m, 8H, -CH_2-), 1.88 (m, 2H, C-CH_2-C), 1.13 [s, 9H, $C(CH_3)_3$]. ^{13}C NMR (D_2O, δ/ppm): 184.22, 180.16, 156.69, 131.11, 130.40, 114.65, 66.90, 62.69, 59.31, 57.28, 46.33, 45.47, 34.29, 28.35, 28.23, 25.76, 16.85. For Re-EC-AMT, the ^{1}H-NMR (D_2O, δ/ppm) result is: 7.02 (d, 2H, phenyl ring), 6.87 (d, 2H, phenyl ring), 4.05 (t, 2H, O-CH_2), 3.17–3.00 (m, 3H, CHN, $PhCH_2$), 2.73–2.50 (m, 8H, -CH_2-), 1.96 (m, 2H, C-CH_2-C), 1.38 (s, 3H, CH_3).

EC-AMT labeled with ^{99m}Tc was achieved with high radiochemical purity (95%) (Fig. 2). The retention time of ^{99m}Tc-EC-AMT matched to that of the cold reference standard Re-EC-AMT (Fig. 2).

In-vitro cellular uptake of ^{99m}Tc-EC-AMT

The cellular uptake kinetics of ^{99m}Tc-EC-AMT, ^{99m}Tc-EC, and FDG using rat breast tumor cells is shown in Fig. 3. The uptake of ^{99m}Tc-EC-AMT into the 13 762 mammary tumor cells initially increased rapidly and reached saturation at 1 h (0.33%). In addition, the %Uptake of ^{99m}Tc-EC-AMT was dramatically higher than that of the negative control, ^{99m}Tc-EC (0.01%), and relatively higher than that of FDG (0.26%).

Competitive inhibition study of ^{99m}Tc-EC-AMT

After incubation with L-tyrosine at 1–100 times as high as the concentrations of EC-AMT and EC, only ^{99m}Tc-EC-AMT and not ^{99m}Tc-EC showed a significantly decreased uptake (Fig. 4). These results indicate that ^{99m}Tc-EC-AMT and L-tyrosine are transported through the same transporter system LAT.

In-vivo tissue distribution studies

The tissue distribution results of ^{99m}Tc-EC-AMT, FDG, and ^{99m}Tc-EC in the normal Fischer 344 rats are shown in Tables 1–3, respectively. Low thyroid uptakes of

Fig. 1

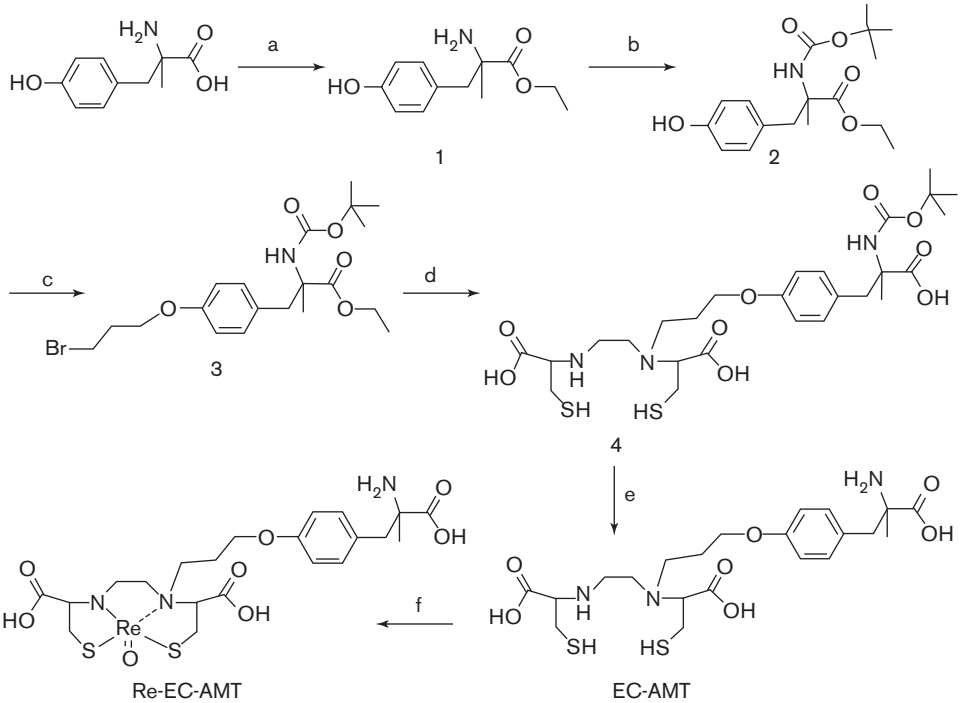

Synthetic scheme of precursor *O*-[3-(*N*-ethylenedicysteine) propyl]-α-methyl tyrosine (EC-AMT) and cold standard reference compound rhenium (Re)-EC-AMT.

Fig. 2

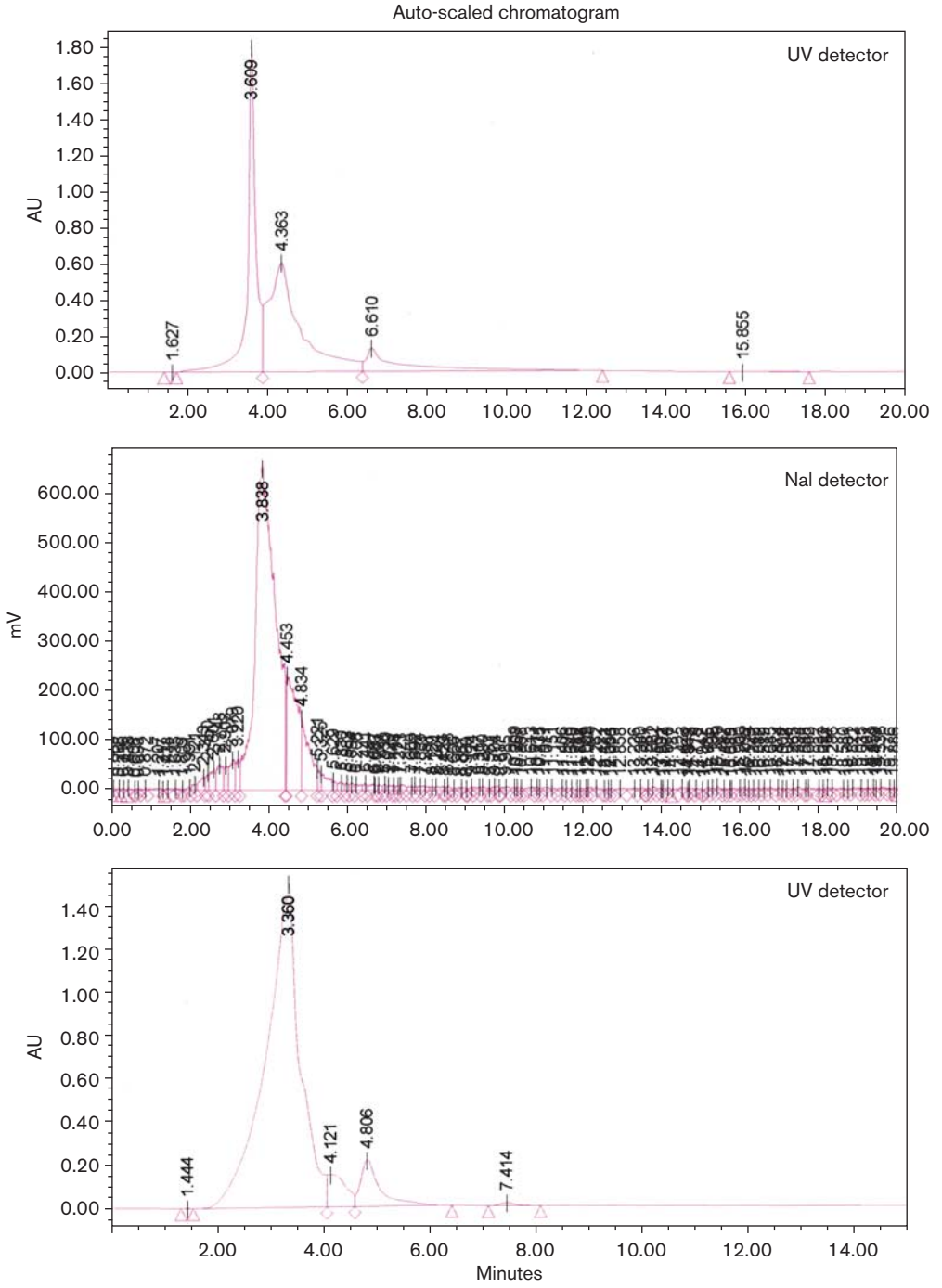

High performance liquid chromatography analysis of technetium-99m *O*-[3-(*N*-ethylenedicysteine) propyl]-α-methyl tyrosine (EC-AMT) and rhenium *O*-[3-(*N*-ethylenedicysteine) propyl]-α-methyl tyrosine (Re-EC-AMT) at a flow rate of 0.5 ml/min using a C-18 reverse column under UV absorbance of 274 nm.

^{99m}Tc-EC-AMT and ^{99m}Tc-EC were observed, suggesting their high stabilities *in vivo* (Tables 1 and 2).

Planar scintigraphic imaging and micro-PET imaging

Planar scintigraphic images of ^{99m}Tc-EC-AMT and ^{99m}Tc-EC control at 30 and 90 min, and the micro-PET image of FDG at 45 min in breast tumor-bearing rats are shown in Fig. 5. T/M ratios of ^{99m}Tc-EC-AMT were 2.72 and 3.31, whereas those of ^{99m}Tc-EC were 1.95 and 1.81, respectively. Tumors could be clearly detected by both ^{99m}Tc-EC-AMT and FDG, but not ^{99m}Tc-EC (Fig. 5).

Fig. 3

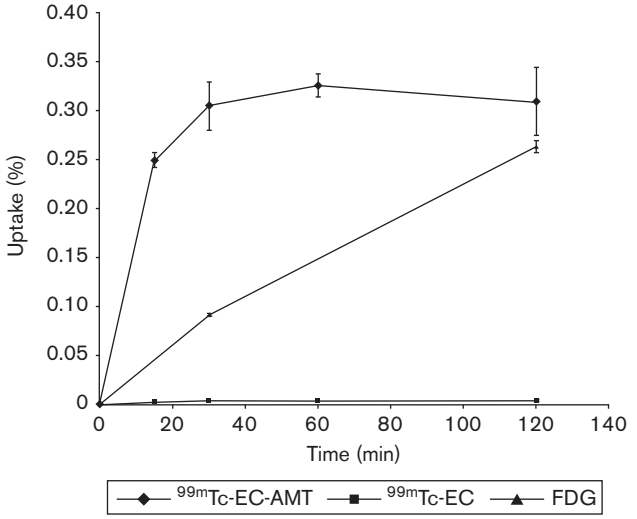

Time course of technetium-99m *O*-[3-(*N*-ethylenedicysteine) propyl]-α-methyl tyrosine (^{99m}Tc-EC-AMT), technetium-99m L,L-ethylenedicysteine (^{99m}Tc-EC) and ^{18}F-2-fluoro-2-deoxy-glucose (FDG) uptake in rat breast tumor cell line 13 762 (0–120 min). Data are expressed in mean ± SD percentage of cellular uptake (%Uptake).

Fig. 4

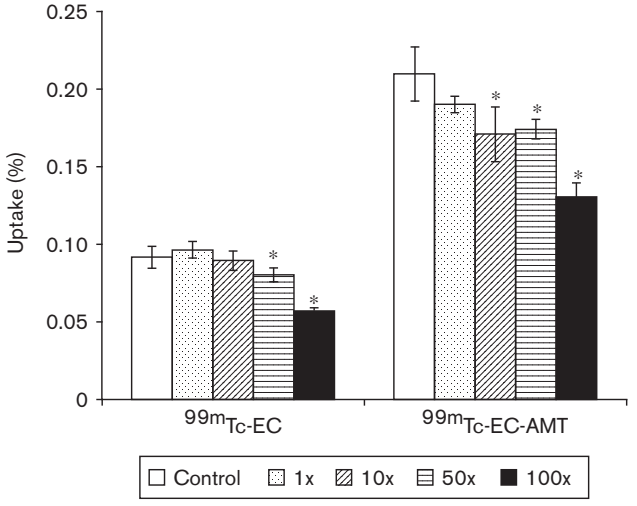

Competitive inhibition of technetium-99m *O*-[3-(*N*-ethylenedicysteine) propyl]-α-methyl tyrosine (^{99m}Tc-EC-AMT) and technetium-99m L,L-ethylenedicysteine (^{99m}Tc-EC) uptake by L-tyrosine in rat breast tumor cell line 13 762 at 60 min. A set of concentrations of L-tyrosine [1x–100x; of ^{99m}Tc-EC-AMT concentration (8 μg/well)] were used. Data are expressed in mean ± SD percentage of cellular uptake (%Uptake). *P < 0.05 compared with the control group.

In-vivo uptake blocking studies

The in-vivo uptake blocking study using unlabeled AMT at 30 and 90 min in breast tumor-bearing rats are shown in Fig. 6. At 30 min, ^{99m}Tc-EC-AMT uptake in the liver, kidney and tumor decreased by 9.8, 47.9 and 23.9%, respectively by using the blocking agent AMT. However, after 90 min, no significant blocking effect was observed. (Results at 4 h are not shown). These results suggest that ^{99m}Tc-EC-AMT uses the same transport system LAT as AMT does, and is taken up by the tumor rapidly.

Table 1 Biodistribution of ^{99m}Tc-EC-AMT in normal Fischer 344 female rats

	30 (min)	60 (min)	240 (min)
Blood	0.64 ± 0.047	0.41 ± 0.019	0.17 ± 0.004
Lung	0.44 ± 0.038	0.29 ± 0.012	0.14 ± 0.004
Liver	2.03 ± 0.180	1.48 ± 0.079	1.07 ± 0.155
Kidney	8.56 ± 0.966	9.01 ± 0.212	8.43 ± 0.171
Stomach	0.28 ± 0.070	0.12 ± 0.006	0.08 ± 0.012
Intestine	0.89 ± 0.107	0.81 ± 0.490	0.13 ± 0.009
Thyroid	0.28 ± 0.029	0.22 ± 0.038	0.09 ± 0.008
Muscle	0.10 ± 0.017	0.05 ± 0.001	0.02 ± 0.001

Each rat received ^{99m}Tc-EC-AMT (25 μCi, intravenously). Each value is percent of injected dose per gram weight (n = 3)/time interval. Each data represents mean of three measurements with standard deviation.
^{99m}Tc-EC-AMT, technetium-99m *O*-[3-(*N*-ethylenedicysteine) propyl]-α-methyl tyrosine.

Table 2 Biodistribution of ^{99m}Tc-EC in normal Fischer 344 female rats

	30 (min)	60 (min)	240 (min)
Blood	0.27 ± 0.039	0.21 ± 0.001	0.15 ± 0.008
Lung	0.19 ± 0.029	0.14 ± 0.002	0.12 ± 0.012
Liver	0.37 ± 0.006	0.29 ± 0.073	0.23 ± 0.016
Kidney	8.99 ± 0.268	9.12 ± 0.053	7.83 ± 1.018
Stomach	0.13 ± 0.106	0.04 ± 0.027	0.04 ± 0.014
Intestine	0.79 ± 0.106	0.40 ± 0.093	0.10 ± 0.009
Thyroid	0.23 ± 0.012	0.11 ± 0.003	0.08 ± 0.005
Muscle	0.04 ± 0.002	0.03 ± 0.009	0.02 ± 0.001

Each rat received ^{99m}Tc-EC (25 μCi, intravenously). Each value is percent of injected dose per gram weight (n = 3)/time interval. Each data represents mean of three measurements with standard deviation.
^{99m}Tc-EC, technetium-99m L,L-ethylenedicysteine.

Table 3 Biodistribution of FDG in normal Fischer 344 female rats

	30 (min)	60 (min)	240 (min)
Blood	0.40 ± 0.042	0.13 ± 0.006	0.06 ± 0.002
Lung	0.55 ± 0.056	0.42 ± 0.024	0.46 ± 0.027
Liver	0.40 ± 0.048	0.16 ± 0.006	0.13 ± 0.012
Kidney	0.71 ± 0.051	0.37 ± 0.012	0.24 ± 0.018
Stomach	0.61 ± 0.078	0.44 ± 0.031	0.39 ± 0.030
Intestine	0.69 ± 0.068	0.53 ± 0.035	0.52 ± 0.025
Thyroid	1.07 ± 0.080	1.04 ± 0.040	1.05 ± 0.069
Muscle	0.33 ± 0.040	0.34 ± 0.027	0.74 ± 0.024

Each rat received FDG (25 μCi, intravenously). Each value is percent of injected dose per gram weight (n = 3)/time interval. Each data represents mean of three measurements with standard deviation.
FDG, ^{18}F-2-fluoro-2-deoxy-glucose.

Discussion

This study investigated the imaging capability of ^{99m}Tc-EC-AMT in breast tumor-bearing rats. In addition, the transport mechanism was examined both *in vitro* and *in vivo*. For chemical synthesis, the precursor EC-AMT was successfully synthesized with an overall yield of 23%. As the chelator EC was unprotected, each EC molecule

Fig. 5

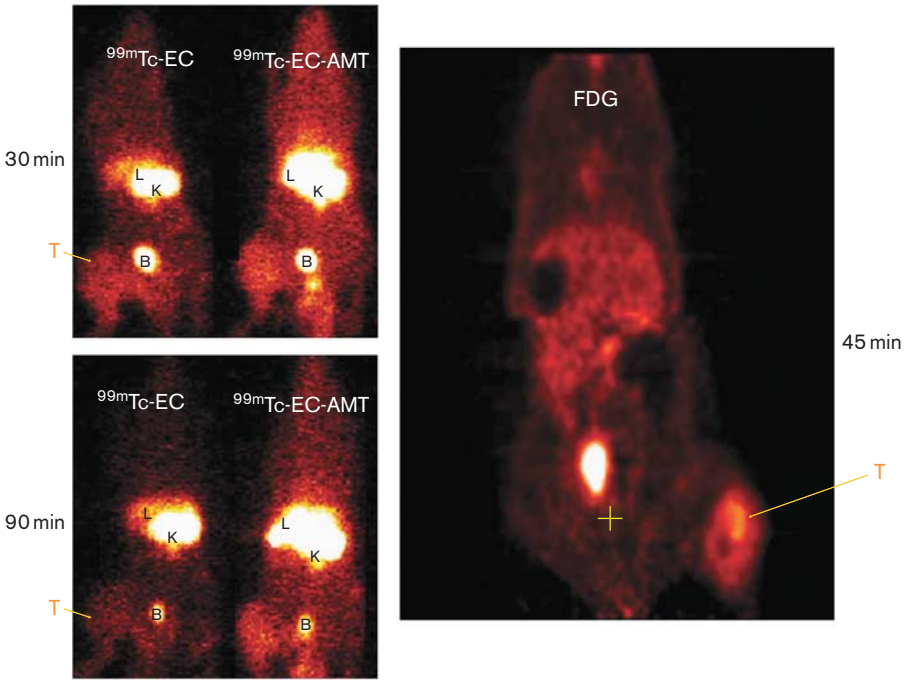

Planar scintigraphy of technetium-99m L,L-ethylenedicysteine (^{99m}Tc-EC) and technetium-99m *O*-[3-(*N*-ethylenedicysteine) propyl]-α-methyl tyrosine (^{99m}Tc-EC-AMT) at 30 and 90 min (left), and micro-PET imaging of ^{18}F-2-fluoro-2-deoxy-glucose (FDG) at 45 min (right) in 13 762 breast tumor-bearing rats. B, bladder; K, kidney; L, liver; T, tumor.

could be conjugated with more than one AMT, and AMT might not only be conjugated with EC specifically on the nitrogen atom but also on the sulfur atom. Those two potential problems could be readily solved by conducting the coupling reaction in the mild aqueous solution instead of the organic one. In addition, the molar ratio of EC and *N*-*t*-butoxycarbonyl-*O*-[3-Br-propyl]-α-methyl tyrosine ethylester (compound 3) was controlled accurately in 2 : 1 under this aqueous solution. Moreover, the structure of EC-AMT could be well confirmed from the ^{1}H-NMR and mass spectra results.

When labeling the precursor EC-AMT with ^{99m}Tc, the radiochemical purity was 95%. With respect to that, ^{99m}Tc-EC-AMT is a kit-product and can be labeled without any further purification; the radiochemical yield was assumed to be identical to its radiochemical purity (95%). Re-EC-AMT was synthesized as the reference standard for the structural confirmation of ^{99m}Tc-EC-AMT. In the periodic table, Tc is a second-row transition element in group 7 and is placed directly above Re. Hence, the chemistry of Tc and Re is very similar, and they are known to have identical coordination parameters with the same ligands such as AMT [17]. From the HPLC results, the retention time of ^{99m}Tc-EC-AMT matched that of Re-EC-AMT, suggesting that the radiochemical structure of ^{99m}Tc-EC-AMT was correct. In addition, one radioisotope of Re, ^{188}Re, is commonly used for internal radionuclide therapy [21]. ^{188}Re-EC-AMT may have value in the treatment of breast cancer, whereas ^{99m}Tc-EC-AMT can be used to diagnose the cancer and monitor its treatment.

In the cellular uptake study, ^{99m}Tc-EC-AMT was taken up rapidly by 13 762 mammary tumor cells and then reached a plateau (Fig. 3). The percentage of cellular uptake of ^{99m}Tc-EC-AMT was significantly higher than that of the negative control ^{99m}Tc-EC. Although there was no remarkable cellular uptake difference between ^{99m}Tc-EC-AMT and FDG, EC-AMT showed a potential benefit over FDG because it could be chelated with various radioisotopes such as ^{99m}Tc and ^{188}Re for both diagnostic and therapeutic applications. In the competitive inhibition study, only ^{99m}Tc-EC-AMT uptake could be significantly inhibited by L-tyrosine, which indicates that ^{99m}Tc-EC-AMT is transported by the amino acid transporter LAT, as in the case of L-tyrosine. Our findings were consistent with other reported studies regarding radiolabeled tyrosine analogs. For instance, ^{11}C/^{14}C-tyrosine [22], ^{123}I/^{125}I-labeled AMT [13,23], ^{18}F-labeled tyrosine [24], AMT [5], and fluoroethyltyrosine [25] have been proven to be predominantly transported through the amino acid transporter LAT. Increased expression level of LAT has been observed in various types of tumors [15], therefore, upregulated LAT is a suitable target for tumor imaging. At the highest 100 times L-tyrosine concentration, both ^{99m}Tc-EC-AMT and ^{99m}Tc-EC showed a decrease

Fig. 6

(a)

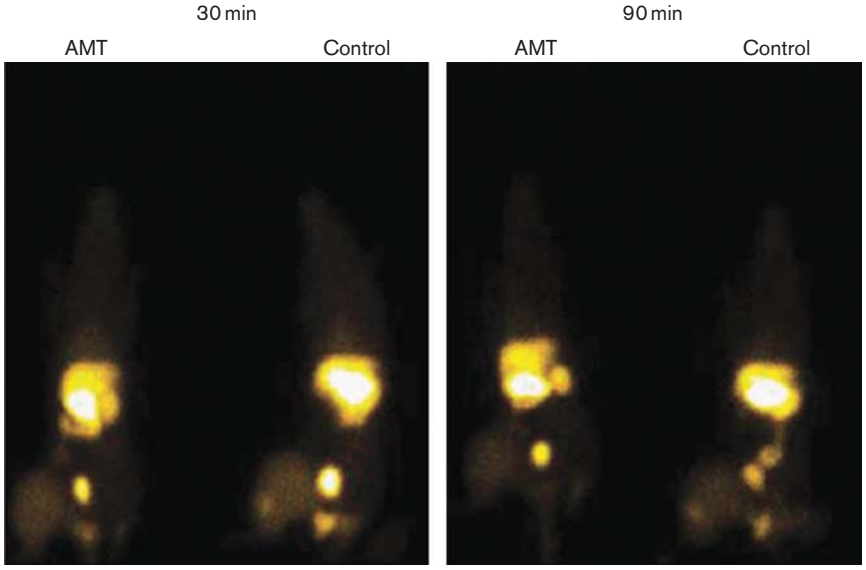

(b)

	30 min		90 min	
	AMT	Control	AMT	Control
Liver/muscle	22.9	25.4	45.8	38.7
Kidney/muscle	53.0	101.8	135.9	165.3
Tumor/muscle	3.5	4.6	3.9	3.7

Effect of unlabeled α-methyl tyrosine (AMT) on tumor and tissue uptake of technetium-99m *O*-[3-(*N*-ethylenedicysteine) propyl]-α-methyl tyrosine (^{99m}Tc-EC-AMT) in mammary tumor bearing-rats. (a) Planar scintigraphy of ^{99m}Tc-EC-AMT with or without AMT (50 mg/kg, intravenously) at 30 and 90 min. (b) Liver/muscle, kidney/muscle and tumor/muscle ratios calculated from the planar scintigraphic images in rats administered with or without unlabeled AMT.

in uptake. This is probably because of cell death caused by the nonspecific cytotoxicity of the extremely high concentration of L-tyrosine.

In planar imaging studies shown in Fig. 5, the organs in the upper abdominal region (liver and kidneys) showed intense activity of ^{99m}Tc-EC-AMT as indicated by arrows. The biodistribution study showed that both ^{99m}Tc-EC-AMT (Table 1) and ^{99m}Tc-EC (Table 2) had high uptake in the liver and kidneys, which was consistent with the results from the imaging study. One possible reason for the high ^{99m}Tc-EC-AMT uptake in kidneys is because of the characteristics of EC given that ^{99m}Tc-EC is known as a renal tubular imaging agent [26]. In addition, Moore *et al.* [27] reported that AMT itself, an inhibitor of tyrosine hydroxylase, could not be excreted from kidneys, and hence crystallized in the proximal tubules because of its poor solubility at the hydrogen ion concentrations of body fluids (pH 5-8). Furthermore, Shikano *et al.* [28] confirmed that the uptake of ^{123}I-labeled AMT ([^{123}I] IMT) into normal human renal proximal tubule epithelial cells could be significantly inhibited by BCH, an LAT specific inhibitor. This result suggests that LAT is involved in [^{123}I] IMT uptake in kidneys. To ascertain whether ^{99m}Tc-EC-AMT uptake is mediated specifically by LAT, we then conducted the similar in-vivo uptake blocking studies using the unlabeled AMT as the competitive inhibitor (Fig. 6). ^{99m}Tc-EC-AMT uptake in the liver, kidney, and tumor were significantly blocked by unlabeled AMT at early time points, which suggested that both ^{99m}Tc-EC-AMT and unlabeled AMT were rapidly taken up through the amino acid transporter LAT *in vivo*. A planar imaging study in the breast tumor-bearing rats was performed at 30–240 min. As there was no marked difference in tumor uptake after 90 min, images at only 30 and 90 min are displayed in Fig. 5. In-vivo uptake blocking study showed that the uptake of ^{99m}Tc-EC-AMT in tumors could be blocked by AMT, and thus decreased at 30 min, but then recovered at 90 min (Fig. 6), suggesting that the best time point for imaging was 30–90 min. With respect to that, the half-life of ^{99m}Tc is 6.02 h; therefore, studies after 6 h will not be clinically practical because of the lack of radioactivity.

Our preliminary results indicate that ^{99m}Tc-EC-AMT is suitable for imaging of breast tumors. By taking the advantages of the coordination capability of the chelator, EC-AMT could chelate various radioisotopes for both imaging and therapy, whereas FDG and other existing amino acid-based radiotracers could not. Further studies to test the specificity of ^{99m}Tc-EC-AMT in differentiating tumors from inflammatory tissues and distinguishing tumors between before and after chemo/radiation therapy will be conducted in the future.

Conclusion

In summary, EC-AMT was synthesized and labeled with ^{99m}Tc readily and efficiently with high radiochemical purity. In-vitro cellular uptake study showed that ^{99m}Tc-EC-AMT transport involved the amino acid transporter system LAT. On account of its simple chemical synthesis, cost effectiveness of the isotope, and planar imaging with comparatively high T/M uptake ratios, ^{99m}Tc-EC-AMT has the potential for tumor imaging and prediction of tumor response to chemo/radiotherapy.

Acknowledgements

This study was supported in part by sponsored research agreement made by Cell > Point L.L.C (MDA LS01-212) and the John S. Dunn Foundation. The NMR, mass spectrometry and animal research were supported by M.D. Anderson Cancer Center (CORE) Grant NIH NCI CA-16672.

References

1 Delbeke D, Coleman RE, Guiberteau MJ, Brown ML, Royal HD, Siegel BA, *et al.* Procedure guideline for tumor imaging with ^{18}F-FDG PET/CT 1.0. *J Nucl Med* 2006; **47**:885–895.

2 Strauss LG. Positron emission tomography: current role for diagnosis and therapy monitoring in oncology. *Oncologist* 1997; **2**:381–388.

3 Chang JM, Lee HJ, Goo JM, Lee HY, Lee JJ, Chung JK, *et al.* False positive and false negative FDG-PET scans in various thoracic diseases. *Korean J Radiol* 2006; **7**:57–69.

4 Rosenbaum SJ, Lind T, Antoch G, Bockisch A. False-positive FDG PET uptake: the role of PET/CT. *Eur Radiol* 2006; **16**:1054–1065.

5 Urakami T, Sakai K, Asai T, Fukumoto D, Tsukada H, Oku N. Evaluation of O-[(18)F]fluoromethyl-d-tyrosine as a radiotracer for tumor imaging with positron emission tomography. *Nucl Med Biol* 2009; **36**:295–303.

6 Langen KJ, Muhlensiepen H, Holschbach M, Hautzel H, Jansen P, Coenen HH. Transport mechanisms of 3-[^{123}I]iodo-alpha-methyl-L-tyrosine in a human glioma cell line: comparison with [^{3}H]methyl]-L-methionine. *J Nucl Med* 2000; **41**:1250–1255.

7 Miyagawa T, Oku T, Uehara H, Desai R, Beattie B, Tjuvajev J, *et al.* Facilitated amino acid transport is upregulated in brain tumors. *J Cereb Blood Flow Metab* 1998; **18**:500–509.

8 Lindstrom LH, Gefvert O, Hagberg G, Lundberg T, Bergstrom M, Hartvig P, *et al.* Increased dopamine synthesis rate in medial prefrontal cortex and striatum in schizophrenia indicated by L-(beta-^{11}C) DOPA and PET. *Biol Psychiatry* 1999; **46**:681–688.

9 Kersemans K, Bauwens M, Mertens J. Method for stabilizing non carrier added 2-[(18)F]fluoromethyl-l-phenylalanine, a new tumour tracer, during radiosynthesis and radiopharmaceutical formulation. *Nucl Med Biol* 2008; **35**:425–432.

10 Inoue T, Shibasaki T, Oriuchi N, Aoyagi K, Tomiyoshi K, Amano S, *et al.* 18F alpha-methyl tyrosine PET studies in patients with brain tumors. *J Nucl Med* 1999; **40**:399–405.

11 Kaira K, Oriuchi N, Otani Y, Shimizu K, Tanaka S, Imai H, *et al.* Fluorine-18-alpha-methyltyrosine positron emission tomography for diagnosis and staging of lung cancer: a clinicopathologic study. *Clin Cancer Res* 2007; **13**:6369–6378.

12 Yamaura G, Yoshioka T, Fukuda H, Yamaguchi K, Suzuki M, Furumoto S, *et al.* O-[^{18}F]fluoromethyl-L-tyrosine is a potential tracer for monitoring tumour response to chemotherapy using PET: an initial comparative in vivo study with deoxyglucose and thymidine. *Eur J Nucl Med Mol Imaging* 2006; **33**:1134–1139.

13 Langen KJ, Pauleit D, Coenen HH. 3-[(123)I]Iodo-alpha-methyl-L-tyrosine: uptake mechanisms and clinical applications. *Nucl Med Biol* 2002; **29**:625–631.

14 Uchino H, Kanai Y, Kim DK, Wempe MF, Chairoungdua A, Morimoto E, *et al.* Transport of amino acid-related compounds mediated by L-type amino acid transporter 1 (LAT1): insights into the mechanisms of substrate recognition. *Mol Pharmacol* 2002; **61**:729–737.

15 Yanagida O, Kanai Y, Chairoungdua A, Kim DK, Segawa H, Nii T, *et al.* Human L-type amino acid transporter 1 (LAT1): characterization of function and expression in tumor cell lines. *Biochim Biophys Acta* 2001; **1514**:291–302.

16 Del Amo EM, Urtti A, Yliperttula M. Pharmacokinetic role of L-type amino acid transporters LAT1 and LAT2. *Eur J Pharm Sci* 2008; **35**:161–174.

17 Jurisson S, Cutler C, Smith SV. Radiometal complexes: characterization and relevant in vitro studies. *Q J Nucl Med Mol Imaging* 2008; **52**:222–234.

18 Marzilli LG. Linking deprotonation and denticity of chelate ligands. Rhenium(V) oxo analogs of technetium-99m radiopharmaceuticals containing N2S2 chelate ligands. *Inorganic Chemistry* 1994; **33**:4850–4860.

19 Yang D, Yukihiro M, Yu DF, Ito M, Oh CS, Kohanim S, *et al.* Assessment of therapeutic tumor response using ^{99m}Tc-ethylenedicysteine-glucosamine. *Cancer Biother Radiopharm* 2004; **19**:443–456.

20 Yang DJ, Ozaki K, Oh CS, Azhdarinia A, Yang T, Ito M, *et al.* (99m)Tc-EC-guanine: synthesis, biodistribution, and tumor imaging in animals. *Pharm Res* 2005; **22**:1471–1479.

21 Iznaga-Escobar N. ^{188}Re-direct labeling of monoclonal antibodies for radioimmunotherapy of solid tumors: biodistribution, normal organ dosimetry, and toxicology. *Nucl Med Biol* 1998; **25**:441–447.

22 Ishiwata K, Vaalburg W, Elsinga PH, Paans AM, Woldring MG. Metabolic studies with L-[1-^{14}C]tyrosine for the investigation of a kinetic model to measure protein synthesis rates with PET. *J Nucl Med* 1988; **29**:524–529.

23 Kawai K, Fujibayashi Y, Yonekura Y, Konishi J, Saji H, Kubodera A, *et al.* An artificial amino acid radiopharmaceutical for single photon emission computed tomographic study of pancreatic amino acid transports ^{123}I-3-iodo-alpha-methyl-L-tyrosine. *Ann Nucl Med* 1992; **6**:169–175.

24 Langen KJ, Jarosch M, Muhlensiepen H, Hamacher K, Broer S, Jansen P, *et al.* Comparison of fluorotyrosines and methionine uptake in F98 rat gliomas. *Nucl Med Biol* 2003; **30**:501–508.

25 Tsukada H, Sato K, Fukumoto D, Kakiuchi T. Evaluation of D-isomers of O-^{18}F-fluoromethyl, O-^{18}F-fluoroethyl and O-^{18}F-fluoropropyl tyrosine as tumour imaging agents in mice. *Eur J Nucl Med Mol Imaging* 2006; **33**:1017–1024.

26 Taylor AT, Lipowska M, Hansen L, Malveaux E, Marzilli LG. ^{99m}Tc-MAEC complexes: new renal radiopharmaceuticals combining characteristics of (99m)Tc-MAG3 and (99m)Tc-EC. *J Nucl Med* 2004; **45**:885–891.

27 Moore KE, Wright PF, Bert JK. Toxicologic studies with alpha-methyltyrosine, an inhibitor of tyrosine hydroxylase. *J Pharmacol Exp Ther* 1967; **155**:506–515.

28 Shikano N, Kawai K, Nakajima S, Nishii R, Flores LG II, Kubodera A, *et al.* Renal accumulation and excretion of radioiodinated 3-iodo-alpha-methyl-L-tyrosine. *Ann Nucl Med* 2004; **18**:263–270.